

Fig. 2. Histochemical study of RE- and PT-treated liver. The left lobes of sample treated liver were sectioned and stained with HE and PAS. (A) RE-, PV-, PV + PT1- (PT 1.0 μ g/ml), PV + PT5- (PT 5.0 μ g/ml), and SA-treated liver were stained with HE. (B) Sectioned samples were stained with PAS plus HE and analyzed at low (upper panel) and high (lower panel) magnification.

RE-treated samples (1 day after RE administration, RE/1d) showed cluster different from others (Fig. 3A). We identified top 150 genes exhibiting the highest scores whose expression was either increased or decreased by RE-administration at day 1 (RE-1d in Fig. 3B). Of those genes, 61 are related to metabolism, 21 encode signal transduction molecules, and the rest are classified as toxic response-, inflammation-, and human-disease-related genes (Fig. 3C). Functions of about one-third of these 150 genes are unknown.

3.4. Identification of toxicity-specific genes

To identify toxicity-related genes from the microarray data, we compared results from RE-treated samples with SA-treated ones. Agp, S100a8, Phyh, Got1, Lbp, and Hpx genes showed the greatest increase in expression level in RE-treated samples (Table 1). When PT-treated animal samples were compared with PV-treated ones, expressions of Hpx, Acmsd, Tat, and Cyp8b1 were significantly increased (Table 1). Phyh, Got1, Acmsd, Tat, and Cyp8b1 participated in metabolism. On the other hand, Agp, S100a8, Lbp, and Hpx participated in inflammation. To quantify expression of candidate genes, the liver cDNAs were analyzed by quantitative RT-PCR (Fig. 4, lower panel), and compared with the microarray data (Fig. 4, upper panel). Liver cDNA were prepared from two or three rats, and two independent quantification experiments were performed. Agp and Hpx genes demonstrated high expression in RE- and PT-treated liver, and their expression was low in PV- and SA-treated liver (Fig. 4). Both were then chosen for further quantitative analysis.

3.5. Agp and Hpx expression in the liver

For confirmation, we performed *in situ* hybridization and immunohistochemistry. Specific probes against Agp clearly detected Agp mRNA in RE-treated liver at day 1 (Fig. 5G and H). Western blot analysis of the cell lysates showed markedly increase of AGP expression in RE-treated liver in comparison with SA-treated liver (Fig. 5Q). Strong AGP protein expression was also detected in RE-treated livers in comparison to SA-treated livers (Fig. 5R–U). From these data, we conclude that AGP is induced in liver by RE-treatment. Since there is no appropriate antibody against rat Hpx, we analyzed Hpx expression by *in situ* hybridization. Hpx expression was rapidly induced in hepatocytes following RE-treatment, and its expression pattern was similar to Agp (Fig. 5I–P). Thus, of the nine genes identified by microarray analysis, histological analysis with specific RNA probes and antibodies demonstrated the highest correlation with Agp and Hpx. Thus, we identify Agp and Hpx as toxicity-related genes and suggest that these genes could be used as biomarkers.

3.6. Detection of PT activity using Q-PCR analysis

To detect alterations in Agp and Hpx gene expressions after vaccine-treatment, we injected various concentrations of PT (0.008–5.0 μ g/ml) and RE into rats. Three rats per group were analyzed. As shown in Fig. 6, expression of Agp and Hpx was tremendously high in RE-treated livers, and both genes showed a strict dependence on the concentration of PT. These genes were clearly up-regulated by PT at

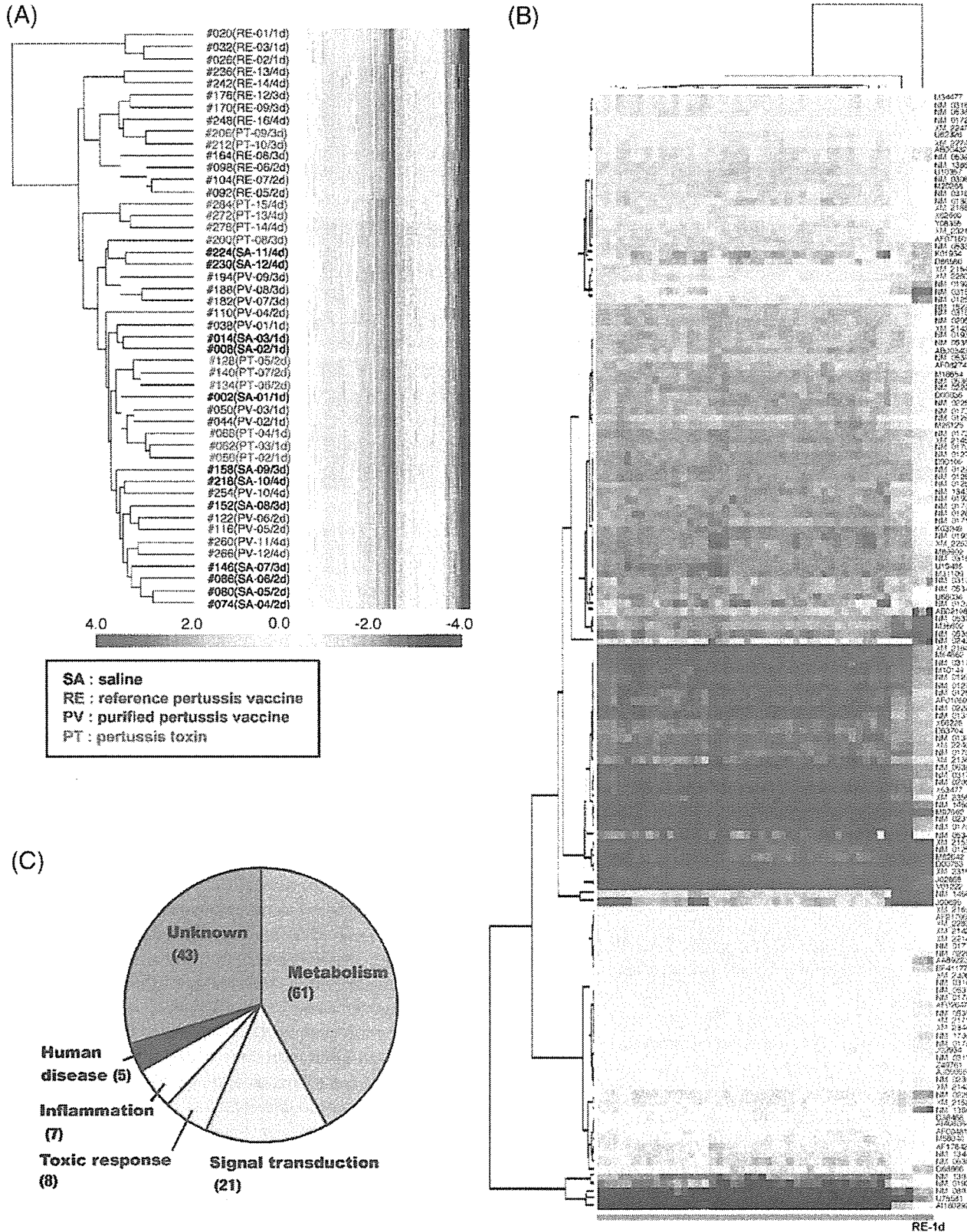


Fig. 3. Gene expression profiles obtained from RE-, PT-, PV-, and SA-treated rats. (A) Genes expressed in sample-treated liver are assembled in the order obtained from the results of cluster analysis. The color bar at left shows the expression ratio vs. the common reference RNA in log₂; red and blue indicate increases and decreases in the expression ratio, respectively. (B) One hundred and fifty genes represented showed significant alterations in RE-treated liver at day 1 (RE-1d). The expression pattern of the 150 genes in other samples (pink bar) showed a clear difference from RE-1d (green bar). The y-axis of the dendrogram depicts the Euclid square distance as the dissimilarity coefficient. Red and blue indicate increases and decreases in the expression ratio, respectively. (C) Genes are classified in the circle graph.

Please cite this article in press as: Hamaguchi I, et al. Two vaccine toxicity-related genes Agp and Hpx could prove useful for pertussis vaccine safety control. Vaccine (2007), doi:10.1016/j.vaccine.2006.12.059

Table 1
Transcripts upregulated in RE- and PT-treated samples

Accession no.	Symbol	Definition	Molecular function	Expression ratios			
				SA	PV	PT	RE
AB018596	Cyp8b1	Rattus norvegicus mRNA for sterol 12-alpha hydroxylase, complete code	Metabolism	1.76 ± 0.15	1.86 ± 0.48	2.70 ± 0.40	3.61 ± 0.96
J00696	Agp/Orm1	Rat alpha1-acid glycoprotein (AGP) mRNA, complete cds	Inflammation	1.34 ± 0.67	1.58 ± 0.36	4.11 ± 0.38	6.30 ± 0.17
M62642	Hpx	Rat (clone pRHx1) hemopexin mRNA, complete cds	Inflammation	2.74 ± 0.37	2.82 ± 0.15	4.08 ± 0.23	5.30 ± 0.07
NM_012571	Got1	Rattus norvegicus glutamate oxaloacetate transaminase 1 (Got1), mRNA	Metabolism	0.11 ± 0.34	0.18 ± 0.24	1.12 ± 0.35	2.86 ± 0.53
NM_012668	Tat	Rattus norvegicus tyrosine aminotransferase (Tat), mRNA	Metabolism	2.55 ± 0.16	2.34 ± 0.58	3.06 ± 0.41	4.18 ± 0.55
NM_017208	Lbp	Rattus norvegicus lipopolysaccharide binding protein (Lbp), mRNA	Inflammation	1.49 ± 0.24	1.47 ± 0.18	3.59 ± 0.41	4.84 ± 0.17
NM_053674	Phyh	Rattus norvegicus phytanoyl-CoA hydroxylase (Phyh), mRNA	Metabolism	2.03 ± 0.19	2.08 ± 0.12	3.22 ± 0.37	3.78 ± 0.16
NM_053822	S100a8	Rattus norvegicus S100 calcium binding protein A8 (calgranulin A) (S100a8), mRNA	Inflammation	-5.94 ± 0.03	-5.89 ± 0.23	-5.25 ± 0.30	-3.07 ± 0.29
NM_134372	Acmsd	Rattus norvegicus 2-amino-3-carboxymuconate-6-semialdehyde decarboxylase (acmsd), mRNA	Metabolism	2.50 ± 0.42	2.10 ± 0.21	3.32 ± 0.84	4.04 ± 0.40

Cyanine 5-labeled liver RNA and Cyanine 3-labeled rat common reference RNA were competitively hybridized to microarrays. Hybridization signals were processed into primary expression ratios ([Cyanine 5-intensity obtained from each sample]/[Cyanine 3-intensity obtained from common reference RNA]), and normalized (primary expression ratios). The primary expression ratios were converted into log₂ values (log₂ Cyanine-5 intensity/Cyanine-3 intensity) as described in Section 2. Log₂ values for each sample were taken an average and calculated S.D.

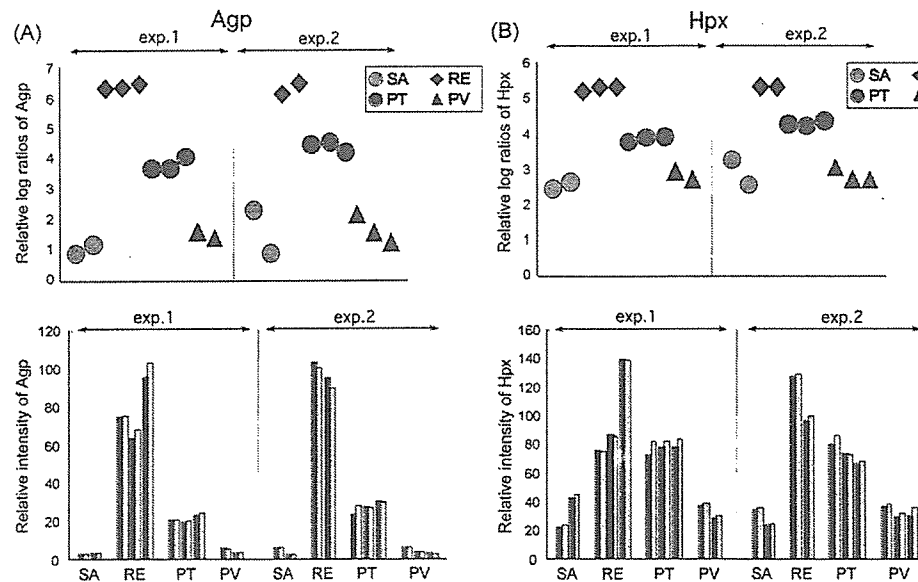


Fig. 4. Comparison of microarray data and quantitative PCR analysis. Expression of Agp (A) and Hpx (B) from DNA microarray analysis (upper panel) is compared with real-time quantitative PCR data (lower panel). (Upper panels) Relative log₂ ratios were extracted from the secondary data matrix for Agp and Hpx. Each symbol represents data from individual animals. Two independent experiments in microarray analysis are shown. (Lower panels) Quantitative PCR analysis of treated livers from individual animals is shown. Duplicate data from each animal is shown as black and white bars. Agp and Hpx expression was assessed relative to rat β -actin.

concentrations of 5 μ g/ml ($P < 0.05$) in comparison with SA, PV, and PT (0.008–0.2 μ g/ml). At concentration of 1 μ g/ml, some animals showed slight high expression of these genes in comparison with the animals treated with SA, PV or PT (0.008–0.2 μ g/ml). These findings suggest that Agp and Hpx may be good candidates to monitor the PT-induced toxicity.

4. Discussion

In this study, we identified genes whose expression is affected by PT-related toxicity using DNA microarray analysis. Although the principle of nucleic acid hybridization is not new, microarrays have opened the way for parallel

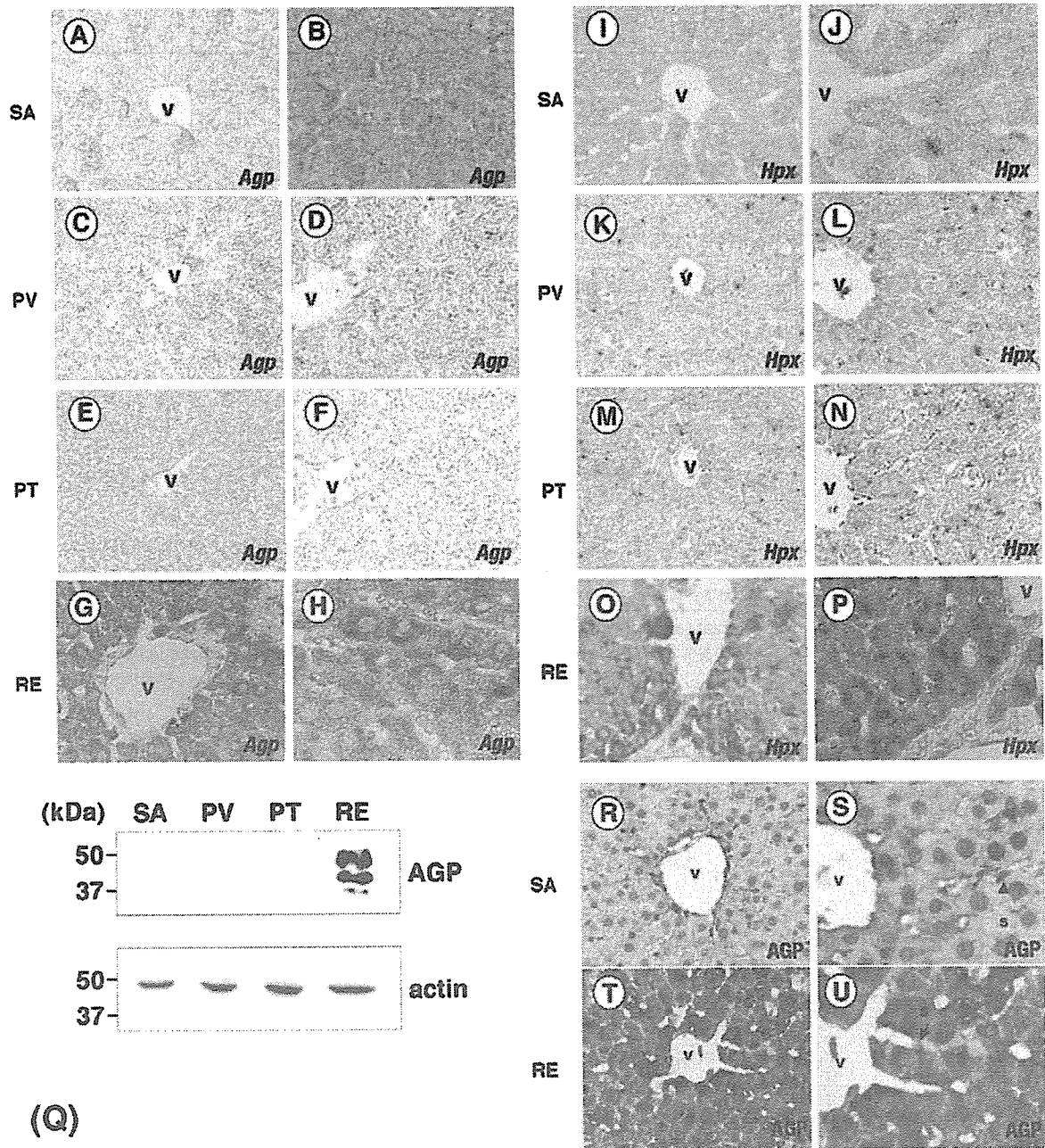


Fig. 5. Expression of Agp and Hpx in RE-, PT-, PV-, and SA-treated liver. Expression of Agp mRNA analyzed by *in situ* hybridization. SA-, PV-, PT-, and RE-treated liver was analyzed at low (A, C, E, and G) and high (B, D, F, and H) magnification. (Q) AGP protein expression in the liver was analyzed by Western blotting. (R–U) Expression of AGP protein in the liver was analyzed by immunohistochemistry. The nuclei were stained with hematoxylin (blue). SA-treated liver was analyzed at low (R) and high (S) magnification. RE-treated liver was analyzed at low (T) and high (U) magnification. Brown indicated AGP protein expression. (I–P) Expression of Hpx mRNA in liver analyzed by *in situ* hybridization. Sections of SA-, PV-, PT-, and RE-treated liver were hybridized with Hpx-specific probes and analyzed at low (I, K, M, and O) and high (J, L, N, and P) magnification. Brown signals represent Hpx expression.

detection and analysis of expression patterns of thousands of genes in a single experiment, and its sensitivity allows detection of subtle differences otherwise difficult to detect. In addition, DNA microarray-based approaches allow us to interrogate toxin-related genomes without bias as to which genes might be altered in expression.

Our histological study showed that RE-treatment severely decreased PAS-stained glycogen granules in hepatocytes.

Since hepatocytes are normally full of such granules, their loss suggests a severe load of toxic substances in liver cells [17]. As liver is a major detoxifying organ and analysis of pharmaceutical toxicity using the DNA array has been undertaken in liver [18], we considered liver an appropriate organ to analyze biological alterations with pertussis vaccine.

Based on analysis of 10,490 of rat genes, we identified 150 genes demonstrating significant changes either upward

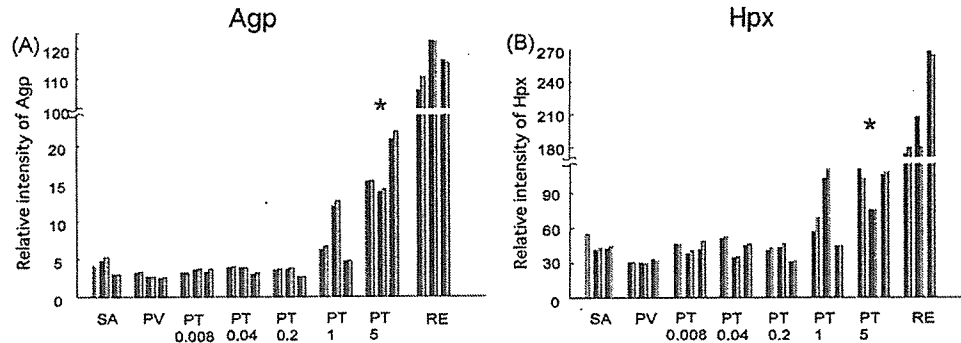


Fig. 6. Quantitative PCR analysis of Agp and Hpx expression in RE-, PT-, PV-, and SA-treated liver. Gene expression of Agp (A) and Hpx (B) in liver treated with various concentrations of PT and RE were analyzed by Q-PCR. Agp and Hpx expression was assessed relative to rat β -actin. Duplicate data from each animal is shown as black and white bars. Three animals per group were analyzed. PT0.008, PT 0.008 μ g/ml; PT0.04, PT 0.04 μ g/ml; PT0.2, PT 0.2 μ g/ml; PT1, PT 1.0 μ g/ml; PT5, PT 5.0 μ g/ml. Asterisk denotes significant differences ($P < 0.05$) by the Student's t -test.

or downward in gene expression after RE-treatment. Among them, several metabolism-related genes, such as FABP (fatty acid-binding protein; U7558) and NaCT (Na⁺-coupled citrate transporter; NM_170668) showed the great increase in expression level. FABP participates in the uptake, intracellular metabolism and/or transport of long chain fatty acids. NaCT plays a role in cellular utilization of citrate in blood for the synthesis of fatty acids and cholesterol and for the generation of energy. The great increase of these genes may be correlated to the toxin-related state of starvation that requires urgent energy derived from fatty tissues.

Reduction in PAS-positive glycogen granules in the liver (Fig. 2) after RE-treatment is consistent with this finding. Gordon et al. have reported that toxic substrates induce abnormal PAS-staining in liver cells due to reduced glycogen granules [19]. Inflammation-related genes, such as MIF (U62326), AGP (J00695), and IL-1 β (NM_031512) are also up-regulated in RE-treated liver, suggesting that acute inflammation is induced by RE-treatment. In addition, many forms of P450 (NM_19303, M16654, NM_012730, X53477, J02868) are induced in the liver by RE treatment. Comparing gene expression among SA-, PT-, and RE-treated animals, we identified nine genes that were up-regulated in toxic conditions. As shown in Table 1, five genes participated in metabolism, and four genes participated in inflammation. Among them, Agp and Hpx showed unequivocal correlation with RE treatment both in the DNA microarray and histological analysis. AGP is a 41–43 kDa glycoprotein with several activities, such as immunomodulating effects and the ability to bind steroid hormones and other molecules [20,21]. Reportedly, AGP serum concentrations, which remain stable in physiological conditions (about 1 g/l in human and 0.2 g/l in rats), increase several-fold during acute-phase inflammatory reactions and AGP is considered as a major member of the positive acute phase protein family. HPX is a serum glycoprotein with a high affinity for heme, and it is produced by and secreted from the liver. It is also known as a scavenger/transporter of heme [22]. Previous studies indicate that purified HPX is an acute-phase reactant

with serum levels increasing several-fold following experimentally induced inflammation [23,24]. These two genes likely react to RE and PT through acute-phase inflammatory reactions. These findings suggest that these biomarkers may be useful to detect PT-induced toxicity in pertussis vaccines.

So far, conventional leukocytosis promoting tests can detect active PT contamination at concentrations greater than 5 μ g/ml. While PAS staining of glycogen granules in RE-treated hepatocytes was weak, hepatocytes treated with a high concentration of PT (5 μ g/ml) were normally stained with PAS. With our method, we detected Agp and Hpx at a 5 μ g/ml PT and the expression level of both genes was dose dependent on PT concentration (Fig. 6). These findings suggest that the gene expression analysis should be useful to detect the PT activity specifically as well as leukocyte-promoting tests. We could detect the different time course of the toxic effects observed as measured by gene expression analysis and leukocytosis. The specific gene expression of Agp and Hpx were observed at day 1 post-treatment, however the increase in WBC were only observed after 2 days. These findings suggest that new test takes the shorter testing period.

Many manufacturers are improving vaccine quality by new methods, such as by using cultured cell lines. However improvements in quality control are continuously required. Since microarray analysis can cover thousands of genes rapidly, it may revolutionize vaccine safety tests and in doing so increase our understanding of molecular mechanisms underlying vaccine toxicity. Given the small variability among test animals, such an approach could potentially reduce the number of animals assayed, alleviating in part ethical problems related to animal tests, which are important issues for regulators worldwide. This method can be used for safety evaluation of different vaccines, such as the emerging vaccine for high pathogenic influenza. So far, safety assessment of vaccines before licensing requires a long time period. Our present assay, with its high reproducibility and reliability, could considerably shorten that period.

Acknowledgments

The authors thank Dr. Hiroshi Yoshikura for helpful discussion and critical reading of the manuscript. The authors have no conflicting financial interests.

Note about research grants: This work was supported by Grants-in-Aid from the Ministry of Health, Labour and Welfare, Japan.

References

- [1] Bordet J, Gengou D. Le microbe de la coqueluche. *Ann Inst Pasteur* 1909;23:415–9.
- [2] Cone TJ. Whooping cough is first described as a disease suigeneris by Baillou in 1640. *Pediatrics* 1970;46:522.
- [3] Sato H, Sato Y. *Bordetella pertussis* infection in mice: correlation of specific antibodies against two antigens, pertussis toxin, and filamentous hemagglutinin with mouse protectivity in an intracerebral or aerosol challenge system. *Infect Immun* 1984;46(2):415–21.
- [4] Pertussis. In: Atkinson W, Hamborsky J, McIntyre L, Wolfe S, editors. *Epidemiology and Prevention of Vaccine-Preventable Diseases*. 9th ed. Washington DC: Centers for Disease Control and Prevention; 2006. p. 79–96.
- [5] Ministry of Health and Welfare, J.G. *The minimum requirements of biological products of Japan 1986*. Tokyo: Ministry of Health and Welfare; 1986.
- [6] Horiuchi Y, Takahashi M, Konda T, Ochiai M, Yamamoto A, Kataoka M, et al. Quality control of diphtheria tetanus acellular pertussis combined (DTaP) vaccines in Japan. *Jpn J Infect Dis* 2001;54(5):167–80.
- [7] Iwasa S, Ishida S, Asakawa S, Kurokawa M. Lymphocytosis-promoting factor produced by *Bordetella pertussis*. *Jpn J Med Sci Biol* 1968; 21:363–8.
- [8] Morsel S. Studies on the lymphocytosis induced in mice by *Bordetella pertussis*. *J Exp Med* 1965;121:49–68.
- [9] Cyster JG, Goodnow CC. Pertussis toxin inhibits migration of B and T lymphocytes into splenic white pulp cords. *J Exp Med* 1995;182(2): 581–6.
- [10] Ishida S, Kurokawa M, Asakawa S, Iwasa S. A sensitive assay method for the histamine-sensitizing factor using change in rectal temperature of mice after histamine challenge as a response. *J Biol Stand* 1979;7(1):21–9.
- [11] Sakamoto A, Imai J, Nishikawa A, Honma R, Ito E, Yanagisawa Y, et al. Influence of inhalation anesthesia assessed by comprehensive gene expression profiling. *Gene* 2005;356:39–48.
- [12] Ejiri N, Katayama K, Kiyosawa N, Baba Y, Doi K. Microarray analysis on Phase II drug metabolizing enzymes expression in pregnant rats after treatment with pregnenolone-16alpha-carbonitrile or phenobarbital. *Exp Mol Pathol* 2005;79(3):272–7.
- [13] Toyooka Y, Tsunekawa N, Takahashi Y, Matsui Y, Satoh M, Noce T. Expression and intracellular localization of mouse Vasa-homologue protein during germ cell development. *Mech Dev* 2000;93(1–2): 139–49.
- [14] Fujiwara Y, Komiya T, Kawabata H, Sato M, Fujimoto H, Furusawa M, et al. Isolation of a DEAD-family protein gene that encodes a murine homolog of *Drosophila vasa* and its specific expression in germ cell lineage. *Proc Natl Acad Sci USA* 1994;91(25):12258–62.
- [15] Kobayashi S, Ito E, Honma R, Nojima Y, Shibuya M, Watanabe S, et al. Dynamic regulation of gene expression by the Flt-1 kinase and Matrigel in endothelial tubulogenesis. *Genomics* 2004;84(1):185–92.
- [16] Ito E, Honma R, Imai J, Azuma S, Kanno T, Mori S, et al. A tetraspanin-family protein, T-cell acute lymphoblastic leukemia-associated antigen 1, is induced by the Ewing's sarcoma-Wilms' tumor 1 fusion protein of desmoplastic small round-cell tumor. *Am J Pathol* 2003;163(6): 2165–72.
- [17] Purushotham KR, Lockard VG, Mehendale HM. Amplification of chloroform hepatotoxicity and lethality by dietary chlordecone (kepone) in mice. *Toxicol Pathol* 1988;16(1):27–34.
- [18] Shipkova M, Spielbauer B, Volland A, Grone HJ, Armstrong VW, Oellerich M, et al. cDNA microarray analysis reveals new candidate genes possibly linked to side effects under mycophenolate mofetil therapy. *Transplantation* 2004;78(8):1145–52.
- [19] Gordon GJ, Coleman WB, Hixson DC, Grisham JW. Liver regeneration in rats with retrorsine-induced hepatocellular injury proceeds through a novel cellular response. *Am J Pathol* 2000;156(2):607–19.
- [20] Fournier T, Medjoubi NN, Porquet D. Alpha-1-acid glycoprotein. *Biochim Biophys Acta* 2000;1482(1–2):157–71.
- [21] Nishi K, Sakai N, Komine Y, Maruyama T, Halsall HB, Otagiri M. Structural and drug-binding properties of alpha(1)-acid glycoprotein in reverse micelles. *Biochim Biophys Acta* 2002;1601(2):185–91.
- [22] Tolosano E, Altruda F. Hemopexin: structure, function, and regulation. *DNA Cell Biol* 2002;21(4):297–306.
- [23] Delanghe JR, Langlois MR. Hemopexin: a review of biological aspects and the role in laboratory medicine. *Clin Chim Acta* 2001;312(1–2): 13–23.
- [24] Muller-Eberhard U. Hemopexin. *Methods Enzymol* 1988;163:536–65.

Differential responses of normal human coronary artery endothelial cells against multiple cytokines comparatively assessed by gene expression profiles

Aya Miura^{a,c}, Reiko Honma^b, Takushi Togashi^c, Yuka Yanagisawa^b, Emi Ito^b, Jun-ichi Imai^b, Takao Isogai^{a,d}, Naoki Goshima^e, Shinya Watanabe^b, Nobuo Nomura^{e,*}

^a Graduate School of Life and Environmental Science, University of Tsukuba, 1-1-1 Ten-noudai, Tsukuba, Ibaraki 305-8572, Japan

^b Department of Clinical Informatics, Tokyo Medical and Dental University, 1-5-45 Yushima, Bunkyo-ku, Tokyo 113-8519, Japan

^c Protein Expression Team, Japan Biological Information Research Center, Japan Biological Informatics Consortium, 2-42 Aomi, Koto-ku, Tokyo 135-0064, Japan

^d Reverse Proteomics Research Institute, Kisarazu, Chiba 292-0818, Japan

^e Protein Expression Team, Biological Information Research Center, National Institute of Advanced Industrial Science and Technology, 2-42 Aomi, Koto-ku, Tokyo 135-0064, Japan

Received 24 October 2006; revised 16 November 2006; accepted 17 November 2006

Available online 27 November 2006

Edited by Takashi Gojobori

Abstract Endothelial cells play an important role in terms of biological functions by responding to a variety of stimuli in the blood. However, little is known about the molecular mechanism involved in rendering the variety in the cellular response. To investigate the variety of the cellular responses against exogenous stimuli at the gene expression level, we attempted to describe the cellular responses with comprehensive gene expression profiles, dissect them into multiple response patterns, and characterize the response patterns according to the information accumulated so far on the genes included in the patterns. We comparatively analyzed in parallel the gene expression profiles obtained with DNA microarrays from normal human coronary artery endothelial cells (HCAECs) stimulated with multiple cytokines, interleukin-1 β , tumor necrosis factor- α , interferon- β , interferon- γ , and oncostatin M, which are profoundly involved in various functional responses of endothelial cells. These analyses revealed that the cellular responses of HCAECs against these cytokines included at least 15 response patterns specific to a single cytokine or common to multiple cytokines. Moreover, we statistically extracted genes contained within the individual response patterns and characterized the response patterns with the genes referring to the previously accumulated findings including the biological process defined by the Gene Ontology Consortium (GO). Out of the 15 response patterns in which at least one gene was successfully extracted through the statistical approach, 11 response patterns were differentially characterized by representing the number of genes contained in individual criteria of the biological process in the GO only. The approach to dissect cellular responses into response patterns and to characterize the pattern at the gene expression level may contribute to the gaining of insight for untangling the diversity of cellular functions.

© 2006 Published by Elsevier B.V. on behalf of the Federation of European Biochemical Societies.

Keywords: Cellular response; Endothelial cell; Cytokine; Gene expression; DNA microarray

*Corresponding author. Fax: +81 3 3599 8141.

E-mail address: nnomura@jbirc.aist.go.jp (N. Nomura).

Abbreviations: IL-1 β , interleukin-1 β ; TNF- α , tumor necrosis factor- α ; IFN- β , interferon- β ; IFN- γ , interferon- γ ; OSM, oncostatin M

1. Introduction

Endothelial cells that line the blood vessels are directly exposed to a variety of stimulatory factors in the blood. In the presence of the stimuli, endothelial cells appropriately modulate their responses with respect to the adhesion of leukocytes, vasorelaxation, and immunity and play an important role in maintaining homeostasis [1]. In addition, endothelial cells are also involved in pathological processes such as thrombosis, requisite neovascularization of solid tumors, and atherosclerosis [2–4]. Thus, it is important to understand in detail the responses of endothelial cells to a variety of exogenous factors.

Cytokines are factors that induce a wide range of responses from endothelial cells. It has been difficult to uncover the differences and similarities in the responses of endothelial cells to cytokines comprehensively. The reason is because several cytokines share common signaling pathways consisting of identical receptor subunits and exhibit similar responses to the expression of a small number of genes and to specific cellular phenotypes.

Thus, it should be efficient to comprehensively analyze in parallel multiple cellular responses against exogenous stimuli via an identical platform in order to reveal the molecular mechanism through which the heterogeneity of responses of endothelial cells is rendered against the exogenous factors represented by cytokines. One of the platforms to conduct these analyses in parallel includes comprehensive gene expression profiling with DNA microarrays. So far, several studies have been published on comprehensive analyses for responses of endothelial cells exposed to cytokines [5–7]. These studies consist of identifying genes the expression levels of which altered in an identical or different fashion; such identification is done by comparing the expression profiles obtained from endothelial cells exposed to two or three species of cytokines side by side comparing two samples on an identical microarray directly. Nevertheless, these direct comparisons among two or three species of cytokines should be insufficient to fully understand the differences and similarities in the heterogeneity of cellular responses to cytokines.

Therefore, we sought to minutely dissect the responses of endothelial cells to cytokines with comprehensive gene

expression profiles obtained from normal human coronary artery endothelial cells (HCAECs) that were exposed to the cytokines interleukin-1 β (IL-1 β), tumor necrosis factor- α (TNF- α), interferon- β (IFN- β), interferon- γ (IFN- γ), oncostatin M (OSM), which are involved in a variety of cellular functions and partially share signal transduction pathways [8–10]. We obtained the gene expression profiles with synthetic DNA microarrays containing approximately 22000 species of probes and analyzed them in parallel. Here, we demonstrate that simultaneous analyses of the expression profiles obtained with these five cytokines enabled us to identify genes the expression levels of which altered in single and multiple cytokines-specific manners and to minutely dissect the cellular responses of HCAECs to the cytokines.

2. Materials and methods

2.1. Cells

HCAECs (Product code, CC-2585; Age, 32Y) were purchased from Cambrex Corp. (NJ, USA) and cultured under 5% CO₂ at 37 °C with EGM-2-MV medium (Cambrex Corp.) containing 5% fetal bovine serum (FBS), hydrocortisone, human fibroblast growth factor (hFGF)-B, vascular endothelial growth factor (VEGF), human recombinant insulin-like growth factor (R3-IGF-1), ascorbic acid, human epidermal growth factor (hEGF), and gentamicin/amphotericin B according to the manufacturer's instructions. HCAECs were split at 1:4 with 0.02% EDTA and 0.25% trypsin at a confluent density.

2.2. Cytokine effects on endothelial cells

HCAECs were maintained at the near confluent density 24 h before the exposure experiments and subsequently replaced with fresh media and incubated for another 24 h. At the fully confluent density, HCAECs were exposed to the following cytokines and subsequently incubated for another 24 h: IL-1 β (R&D Systems, MN, USA) (1.1 nM), TNF- α (R&D Systems) (0.3 nM or 10 nM), IFN- β (PeproTech Inc., NJ, USA) (0.03 nM or 1.3 nM), IFN- γ (R&D Systems) (0.04 nM or 0.5 nM), OSM (R&D Systems) (1.1 nM or 2.7 nM). The cells were treated at two different concentrations; one was slightly over the median effective dose (ED₅₀) specified by the manufacturers and other was excessively over the ED₅₀. As negative controls for exposure (mock samples), fresh medium containing no cytokines were added to the culture.

2.3. Poly A(+) RNA preparation

The cells were harvested 24 h after exposure to cytokines with TRIzol Reagent (Invitrogen Corp., CA, USA). The cell lysates obtained were subjected to total RNA extraction according to the manufacturer's instructions. Subsequently, total RNA was subjected to polyA(+) RNA isolation with a MicroPoly(A) Purist Kit (Ambion Inc., TX, USA) in accordance with the manufacturer's instructions. Eventually, polyA(+) RNA was divided into aliquots of 2 μ g, precipitated with ethanol, and stored at -20 °C.

2.4. Preparation of DNA microarrays and acquisition of gene expression profiles

A set of synthetic polynucleotides (80-mers) representing 22512 species of human transcript sequences that are mostly originated from the Reference Sequence (RefSeq) project clones deposited in the National Center for Biotechnology Information (NCBI) database was purchased (MicroDiagnostic, Tokyo, Japan) and printed on a glass slide (coated glass slide for the microarray, type I; Matsunami Glass Ind., Ltd., Kishiwada, Japan) with a custom-made arrayer (designated as the 22K array) [11,12]. Two micrograms of poly(A)+ RNA were labeled with SuperScript II (Invitrogen Corp.) and cyanine 5-deoxyuridine triphosphate (dUTP) (Perkin-Elmer Inc., MA, USA) for each HCAECs sample or cyanine 3-dUTP (Perkin-Elmer Inc.) for a human common reference RNA. The human common reference RNA was prepared by mixing equal amounts of poly(A)+ RNA extracted from 22 cell lines (A431, A549, AKI, HBL-100, HeLa, HepG2, HL60, IMR-32, Jurkat, K562, KP4, MKN7, NK-92, Raji, RD, Saos-2,

SK-N-MC, SW-13, T24, U251, U937, and Y79). Hybridization and subsequent washes of the arrays were performed with a Labeling and Hybridization Kit (MicroDiagnostic). Hybridization signals were measured with a GenePix 4000A scanner (Axon Instruments Inc., Union City, CA) and then processed into primary expression ratios (ratios of cyanine 5 intensity of each sample to cyanine 3 intensity of the human common reference RNA) by the GenePix Pro 3.0 software (Axon Instruments Inc.). Normalization was performed for each ratio by multiplying the normalization factors calculated by the GenePix Pro 3.0 software. The primary expression ratios were converted into log₂ values (designated as log ratios). All the data in accordance with the MIAME guideline were deposited at DDBJ via CIBEX (<http://cibex.nig.ac.jp/index.jsp>) in Accession Numbers CBX14.

2.5. Data analysis

Data processing and subsequent hierarchical clustering analysis were conducted with an MDI gene expression analysis software package (MicroDiagnostic). To compare the cytokine-treated samples against the mock-treated samples (negative controls) for each cytokine, log ratios obtained for the mock-treated samples were subtracted from the log ratios obtained for each cytokine-treated sample (designated as relative log ratios) (Supplementary Table 1). Next, genes, the relative log ratios of which in the two independent samples for each cytokine were greater than 0.75 or smaller than -0.75, were extracted (Supplementary Table 2). In order to obtain data on these extracted genes, they were processed into a matrix (rows, genes; columns, samples) and subjected to two-dimensional hierarchical clustering analysis. Furthermore, for extracting genes that enabled us to distinguish between the two groups of samples in terms of the presence or absence of the expression alteration of interest (designated as the presence group and the absence group, respectively), we calculated a statistical value consisting of the absolute value of the difference between the mean average of relative ratios among the presence group and that among the absence group divided with the sum of the standard deviation of the relative log ratios among the presence group and that among the absence group (designated as signal:noise ratios); this was done for all two-group combinations among the five individual cytokines. Eventually, we extracted genes that revealed signal:noise ratios that were greater than two and absolute values of the relative log ratios for the presence groups that were greater than 0.75.

3. Results

3.1. Acquisition of gene expression profiles

To investigate the heterogeneity of the responses of endothelial cells, which line the blood vessels and are directly exposed to a variety of stimulatory factors in the blood, to cytokine stimulation in terms of alteration in gene expression, we obtained comprehensive gene expression profiles with DNA microarrays containing about 22000 species of probes for human transcripts from HCAECs that were treated for 24 h with the cytokines that are responsible to a variety of cellular functions. In this study, we chose the following five cytokines as models: IL-1 β and TNF- α , both involved in inflammatory responses following infection and tissue damages [13]; IFN- β and IFN- γ principal mediators in immune responses such as antiviral activities and antitumorogenic activities [14,15]; and OSM, involved in accelerative and inhibitory functions in inflammation and in vascularization [16–19]. These cytokines were exposed to HCAECs at two different concentrations in two independent experiments to eliminate the genes in which the expression levels are robustly affected by the differences in the magnitude of stimulation.

3.2. Overview of alteration of gene expression in HCAECs after cytokine stimulation

First, we extracted genes in which both relative log ratios (see Section 2) in two different samples treated with identical

Table 1
The number of genes that exhibited the alteration of expression levels after individual cytokines

Treatment	Upregulated ^a	Downregulated ^b	Total
TNF- α	407	184	591
IL-1 β	181	88	269
IFN- β	121	28	149
IFN- γ	129	28	157
OSM	46	33	79

^aThe number of increased genes that showed relative log ratio greater than 0.75 across two independent samples treated with individual cytokines.

^bThe number of decreased genes that showed relative log ratio smaller than -0.75 across two independent samples treated with individual cytokines.

cytokines were greater than 0.75 or smaller than -0.75; this was done to concentrate only on the genes that were robustly affected by the cytokine stimulation. The numbers of genes extracted under the abovementioned condition were: TNF- α , 591; IL-1 β , 269; IFN- β , 149; IFN- γ , 157; OSM, 79 (Table 1). These results indicate that the most robust influence was induced by TNF- α and the faintest influence was produced by OSM at the gene expression level in HCAECs. Next, to compare the cellular responses in HCAECs at the gene expression level, we generated a data matrix with the genes described above and subjected it to a two-dimensional hierarchical clustering analysis (Fig. 1). The clustering analysis provided five different sample clusters and each cluster consisted of two samples treated with identical cytokines (Fig. 1). Moreover, the TNF- α and IL-1 β clusters formed an identical larger cluster; the IFN- β and IFN- γ clusters generated an identical larger cluster. These two larger clusters produced one of the largest clusters in the dendrogram (Fig. 1). These results are consistent with the previously reported findings that a pair of TNF- α and IL-1 β or that of IFN- β and IFN- γ share similar activities in terms of the alteration of gene expression and functional responses [20,21]. Moreover, we observed that the alteration of gene expression in OSM-treated HCAECs was less robust than those in the other four cytokine-treated cells and that the constituents of the genes in which expression altered after the OSM exposure were less overlapped compared to those found in the other four cytokine-treated samples. Taken together, these findings indicate that a parallel analysis of genes extracted from expression profiles clearly distinguishes the responses in the five cytokine-treated HCAECs in a cytokine-specific manner.

3.3. Identification of genes that shared similar response patterns among the different cytokine-treated samples

For the clustering analysis shown in Fig. 1 in the direction across genes, we paid attention to the presence of genes in which expression altered in multiple and single cytokine-specific manners. The reason is that the response patterns for the alteration of gene expression should reflect the extent of specificity and similarity in the responses of HCAECs against these cytokines. Therefore, we sought to disclose the presence of more minutely heterogeneous response patterns among the five cytokines compared to those brought forth by the hierarchical clustering analysis (as shown in Fig. 1) and to identify the genes included in the response patterns. For this advanced purpose, we extracted genes from the data matrix of relative

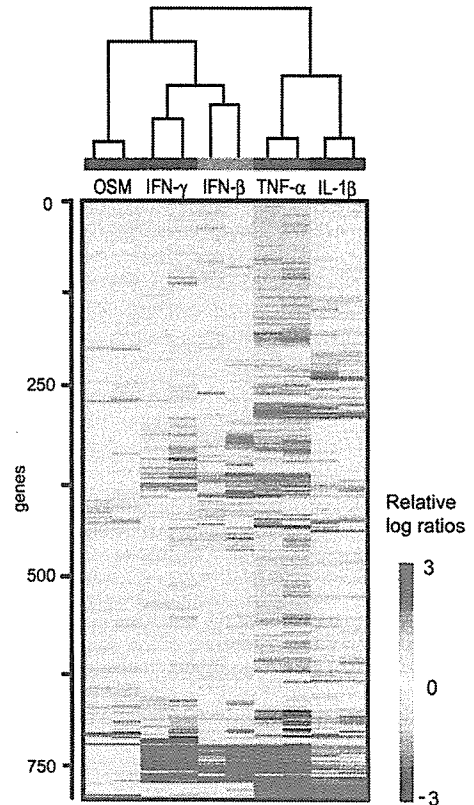


Fig. 1. Comparison of gene expression profiles obtained from HCAECs stimulated with cytokines. Robustly expressed genes after stimulation with IL-1 β , TNF- α , IFN- β , IFN- γ , and OSM were extracted and subjected to two-dimensional hierarchical clustering analysis. Columns and rows indicate samples (10) and genes (789), respectively. Genes and samples are aligned in the order defined by the results of the clustering analysis. The dendrogram indicates the relationship among the samples based on dissimilarity coefficients calculated through the clustering analysis. The color bar at the bottom of the figure represents the grades of the relative expression levels: increase, red; decrease, blue. Each color box under the dendrogram at the top of the figure depicts an individual cytokine: IL-1 β , blue; TNF- α , orange; IFN- β , pink; IFN- γ , green; OSM, violet. All the relative log ratios included in this figure are shown in Supplementary Table 2.

log ratios by another statistical procedure; these genes were included in all the two-group combinations of the five cytokines (see Section 2).

The statistical extraction provided 15 species, each with distinct patterns (designated as response patterns) (Table 2). Out of these 15 patterns, 10 response patterns were common to multiple cytokines (response patterns A, B, C, D, I, J, K, L, M, and N), whereas five response patterns were solely specific to a single cytokine for all the five cytokines tested (response patterns E, F, G, H, and O). Among the response patterns solely specific to individual cytokines, the most prominent response pattern was observed in a TNF- α -specific manner as response pattern E consisting of 95 genes. On the other hand, the most quiescent response pattern was seen in an IFN- β -specific manner as response pattern O consisting of one gene (Table 2).

The extracted 15 response patterns included identical genes in duplicate across two response patterns. Response patterns D and J included *PLSCR1* in which expression increased

Table 2
Response patterns and the number of genes included in the response patterns

Response pattern	TNF- α	IL-1 β	IFN- β	IFN- γ	OSM	Genes ^a
A	+	+	+	+		39
B	+	+				55
C	+		+	+		9
D	+		+			7
E	+					95
F		+				28
G				+		19
H					+	10
I	+		+	+	+	1
J		+		+	+	1
K	+	+		+		1
L	+			+		1
M	+				+	1
N		+			+	1
O			+			1

Notes: +, the presence of alteration (a constituent of the presence group). Blank: the absence of alteration (a constituent of the absence group). The meaning of alteration is as follows: (i) in the presence group, the absolute value of the relative log ratio was greater than 0.75 for both of the two independent samples treated with individual cytokines; (ii) the absolute value of the difference in the mean average of the relative ratios divided by the sum of the standard deviation of the relative ratios among each group for individual cytokines was greater than 2.

^aThe number of genes constituting each response pattern.

after stimulation with all five cytokines. Response patterns B and E included five genes (*LTB*, *LAMC2*, *TNFAIP3*, *SDC-CAG28*, and *D6S49E*) in common; response patterns B and F included four genes (*CLU*, *SCYB5*, *SART-2*, and *MYO1B*) in common (all the full names of the genes are shown here and below, while abbreviations are listed in Supplementary Table 2).

Moreover, seven response patterns contained a single gene as the constituent (response patterns I, J, K, L, M, N, and O). These response patterns involved *PLSCR1* in response pattern J, *GAGED2* in response pattern I, *TNFAIP2* in response pattern K, *AKR1C3* in response pattern L, *LOC58489* in response pattern M, *IER3* in response pattern N, and *COLF6967* in response pattern O (Supplementary Fig. 1). Since these patterns include a single gene only as each constituent, further accumulation of experimental data obtained with a variety of exogenous stimuli to multiple cell species and information on gene ontology should be required to speculate the relevance and biological significance of these patterns.

3.4. Genes in which expression altered similarly in a multiple cytokine-specific manner

To study the kind of cellular responses represented by the response patterns consisting of two and more genes (response patterns A, B, C, D, E, F, G, and H), we analyzed the association between the previously accumulated findings and the individual genes included in the response patterns. First, we confirmed that all the response patterns exhibited the two largest clusters that should clearly distinguish the two groups of interest among all the samples by hierarchical clustering analysis in the direction across the samples (Figs. 2 and 3). Next, for genes encoding for actual proteins among those consisting of these response patterns, we scrutinized the definition of bio-

logical process in Gene Ontology Consortium (GO) (<http://www.geneontology.org/>) edited by Human Protein Reference Database (<http://www.hprd.org/>) [22] and reference information.

These results indicate that the cellular responses of HCAECs include at least four different response patterns defined by the alteration of the expression levels of genes, as shown in Fig. 2, and that each response pattern contains genes that are affected differently by two groups of cytokine, i.e., the group for the presence of influence (the robustly influential group) and the one for the absence of influence (the weakly influential group), which comprises at least two cytokines.

3.5. Genes in which expression levels solely altered in a single cytokine-specific manner

We continued an identical approach to characterize the response patterns comprising genes in which expression levels solely altered in a single cytokine-specific manner.

Fig. 3A shows the response pattern E consisting of genes that exhibited robust alteration only after TNF- α stimulation. Fig. 3B represents the response pattern F consisting of genes that exhibited robust alteration only after IL-1 β stimulation. Fig. 3C displays the response pattern G consisting of genes that exhibited robust alteration only after IFN- γ stimulation. Fig. 3D demonstrates the response pattern H consisting of genes that exhibited strong alteration only after OSM stimulation, including those that showed different expression changes amongst each other in case of both OSM stimulation and IL-1 β and TNF- α stimulation and those that showed alteration only after OSM stimulation.

These results indicate that cellular responses of HCAECs include at least four different response patterns defined by the alteration of expression levels of genes shown in Fig. 3 and that each response pattern contains genes solely affected by a single cytokine. Furthermore, these results suggest the presence of greatly different modulation mechanisms in HCAECs for the OSM stimulation and the IL-1 β and TNF- α stimulation pathways.

3.6. Comparison of 15 response patterns in parallel

Eventually, we sought to characterize all 15 response patterns and compare them to one another by connecting the number of genes belonging to each criterion in the biological process to each response pattern (Table 3). Consequently, we obtained the following findings. Genes that are well characterized in function and involved in immune response following viral and bacterial infections were included abundantly in the response patterns A (12 out of 39; 31%) and G (7 out of 19; 37%) but scarcely in the response patterns E. Genes associated with apoptosis were included in the response patterns A, B, and E. Genes involved in cell growth/maintenance were present in the response patterns B, E, F, and H but absent in the other response patterns. Genes related to protein metabolism were present in the response patterns A, B, C, D, E, and G but absent in the other response patterns. Between the response patterns A and D and the response pattern B, we observed contrastive characteristics with respect to protein metabolism; the response patterns A exhibited an increased expression of constituents belonging to the ubiquitin–proteasome system, including

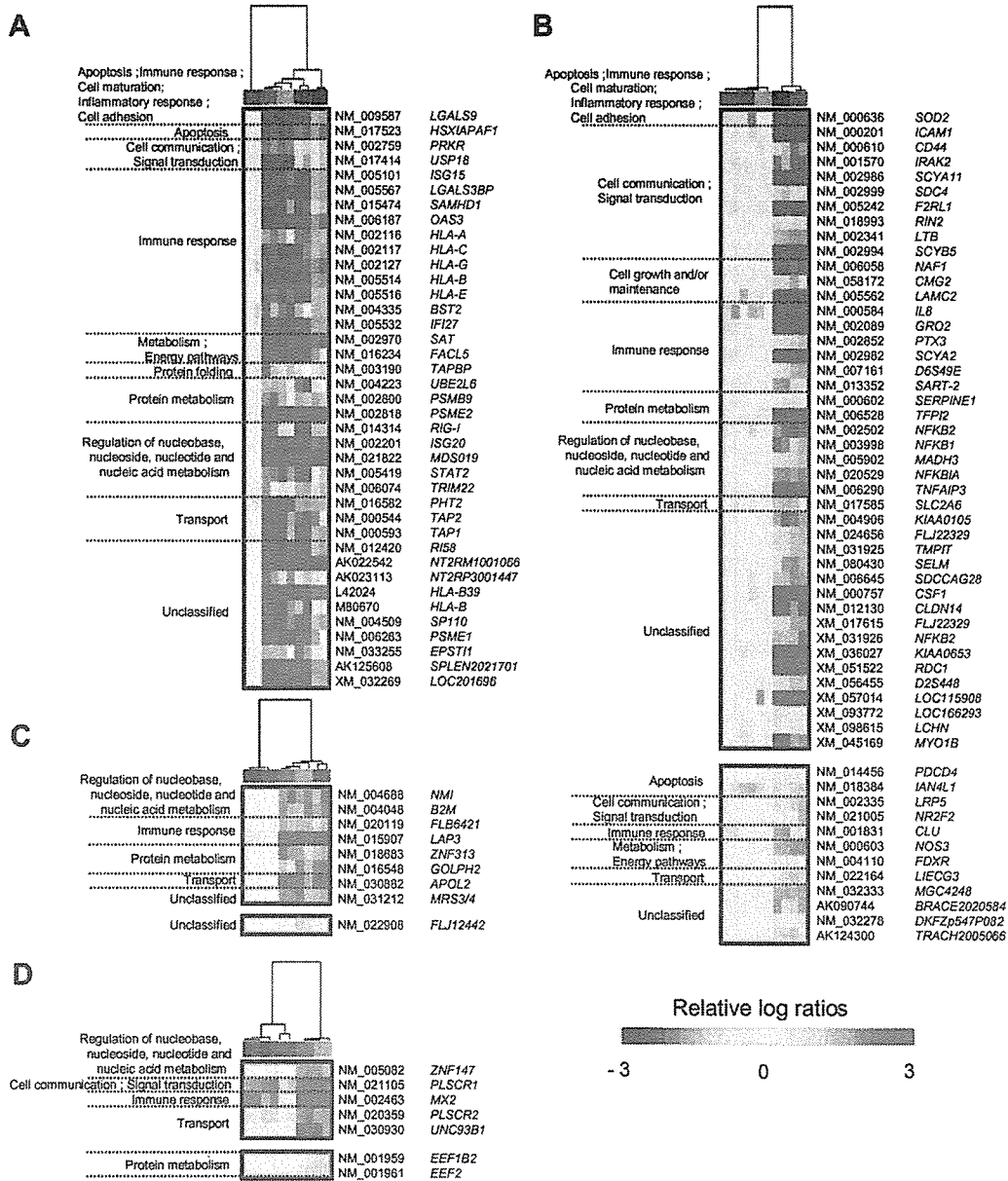


Fig. 2. Genes in which expression levels altered similarly in a multiple cytokine-specific manner. (A) Response pattern A consisting of 39 genes in which expression levels altered similarly after stimulation with TNF- α , IL-1 β , IFN- β , and IFN- γ . (B) Response pattern B composed of 55 genes that exhibited similar alteration of expression levels after stimulation with TNF- α and IL-1 β . (C) Response pattern C comprising nine genes that exhibited similar alteration of expression levels after stimulation with TNF- α , IFN- β , and IFN- γ . (D) Response pattern D containing seven genes in which the expression levels altered similarly after TNF- α and IFN- β stimulation. The color bars at the bottom right of the figure represents the grades of the relative expression levels: increase, red; decrease, blue. Each color box at the top of the figure depicts an individual cytokine: IL-1 β , blue; TNF- α , orange; IFN- β , pink; IFN- γ , green; OSM, violet. At the left side of each panel, the biological process for each gene contained is indicated, which is defined in the Gene Ontology Consortium (<http://www.geneontology.org>). At the right side of each panel, the accession number and gene ID for each gene contained is demonstrated, which is derived from the National Center for Biotechnology Information (NCBI) Reference Sequences (<http://www.ncbi.nlm.nih.gov/RefSeq/>). The full name of each gene is shown in Supplementary Table 2, linked to each Gene ID. All the relative log ratios included in this figure are shown in Supplementary Table 3.

PSMB9 and *PSME2*, and the response pattern D showed the decreased expression of elongation factors, namely, *EEF2* and *EEF1B2*, whereas the response pattern B exhibited an increased expression of an inhibitory factor for proteolysis, *SERPINE1*.

Overall, these results indicate that out of the 15 response patterns in which at least one gene was successfully extracted

through the statistical approach, 11 response patterns were differentially characterized by representing the number of genes contained in individual criteria of the biological process in the GO only. These suggest that the approach to link the genes constituting the response patterns with the biological process defined by the GO may endorse the classification with the response patterns as being biologically meaningful.

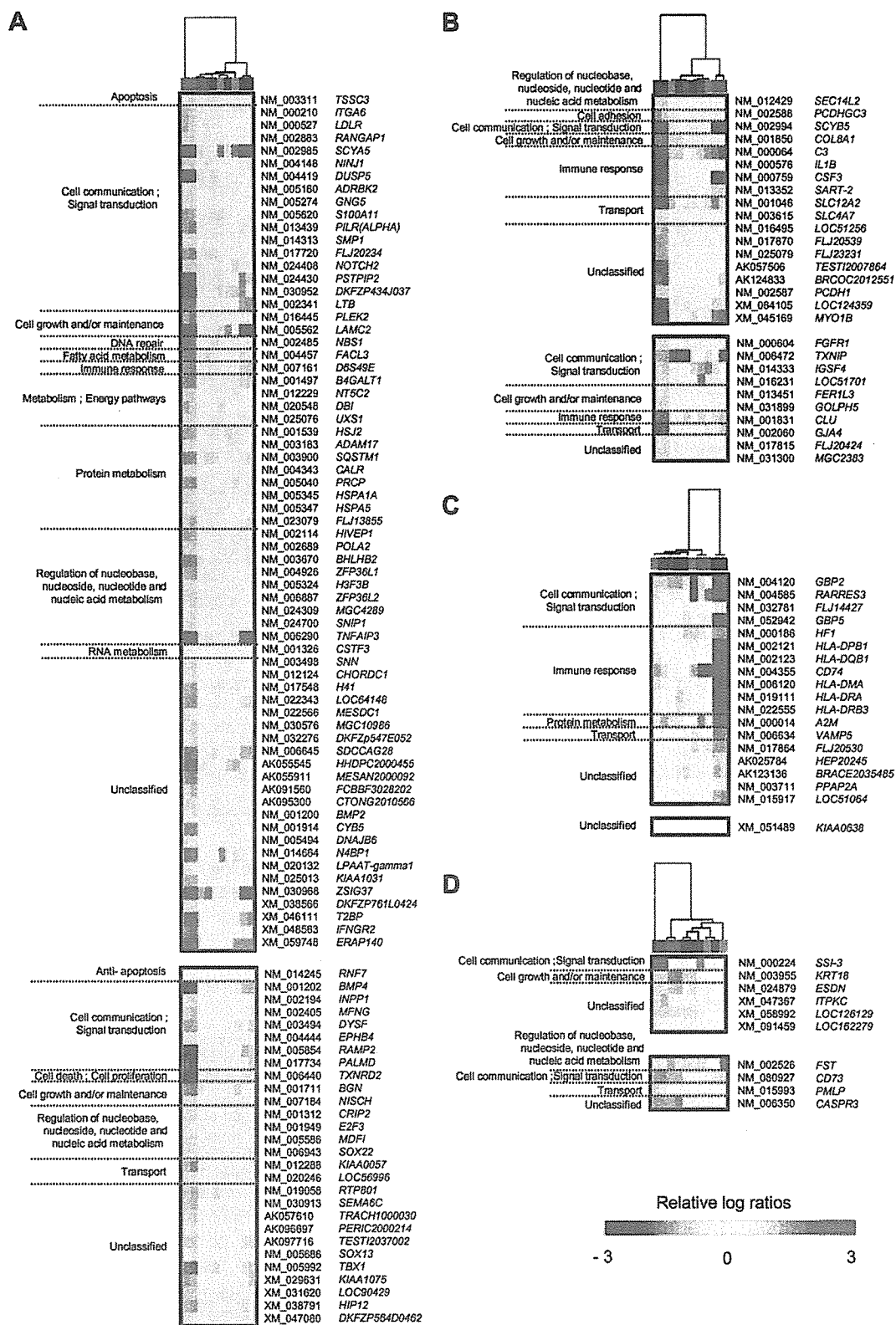


Fig. 3. Genes in which expression levels solely altered in an individual cytokine-specific manner. (A) Response pattern E consisting of 95 genes that exhibited expression alteration only after TNF- α stimulation. (B) Response pattern F comprising 28 genes that demonstrated expression alteration only after IL-1 β stimulation. (C) Response pattern G composed of 19 genes that exhibited expression alteration only after IFN- γ stimulation. (D) Response pattern H consisting of 10 genes that showed expression alteration only after OSM stimulation. All the relative log ratios included in this figure are shown in Supplementary Table 4.

Table 3
Distribution of the number of genes assigned to the major criteria of the biological process defined by the Gene Ontology Consortium (GO)

Biological process ^a	Response pattern														
	A	B	C	D	E	F	G	H	I	J	K	L	M	N	O
Anti-apoptosis					1										
Apoptosis	2	3			1										
Cell adhesion	1	1				1									
Cell communication; signal transduction	2	11		1	23	5	4	2		1					
Cell death					1										
Cell growth and/or maintenance			3		4	3		1							
Cell maturation	1	1													
Cell proliferation					1										
DNA repair					1										
Fatty acid metabolism					1										
Immune response	12	8	2	1	1	5	7								
Inflammatory response	1	1													
Metabolism; energy pathways	2	2			4								1		
Protein folding	1														
Protein metabolism	3	2	2	2	8		1								
Regulation of nucleobase, nucleoside, nucleotide and nucleic acid metabolism	5	5	2	1	13	1			1						
RNA metabolism					1										
Transport	3	2	1	2	2	3	1	1							
Unclassified/biological_process unknown	1	6	1		10	5	5				1				
Unclassified/unannotated	9	14	1		24	5	1	5	1				1	1	1

^aEach gene is assigned to all the corresponding criteria of the biological process defined by GO (<http://www.geneontology.org/>) in a repetitive manner.

4. Discussion

In this study, we compared in parallel the cellular response of HCAECs to the cytokines, such as IL-1 β , TNF- α , IFN- β , IFN- γ , and OSM, which are profoundly associated with the immune and inflammatory reactions in endothelial cells from the standpoint of the comprehensive alteration in gene expression. We conducted two independent approaches to analyze expression profiles obtained from HCAECs stimulated with these cytokines. One was hierarchical clustering analysis done only with genes in which expression levels altered robustly after the stimulation; the other was statistical extraction of the genes of interest from all the profiles divided into all combinations of two groups among five cytokines. Based on the results of the clustering analysis in the direction across samples, we concluded that these genes are responsible for distinguishably classifying these five cytokines at the gene expression level. Moreover, based on the results of the statistical extraction of the genes, we concluded that cellular responses after stimulation with these five cytokines solely described by gene expression ratios were composed of at least 15 patterns (designated as response patterns) (Table 2), identifying genes that constitute the individual response patterns. Eventually, we linked these genes constituting the response patterns with the biological process defined by the GO and endorsed the classification with the response patterns as being biologically meaningful (Table 3).

As an experimental model system to investigate the responses of endothelial cells to a variety of exogenous stimuli, we chose five cytokines associated with inflammation and HCAECs under a flat culture condition. Since HCAECs are reported to exhibit different responses to inflammation cytokines when compared to human umbilical vein endothelial cells and human pulmonary artery endothelial cells in terms of gene expression and protein secretion [23,24], it may be appropriate that the implication of our findings presented here should be

restricted to HCAECs as a model. Further experiments should be required with other subtypes of endothelial cells in addition to different lots of HCAECs under distinct culture conditions such as those that allow endothelial cells to form tubular structures to establish more general implication of endothelial cell responses to the cytokines used in this study. Moreover, although we chose a single time point of 24 h after cytokine exposure since we failed to obtain robust alteration at the gene expression level in preliminary experiments with smaller microarrays at the time point of 4 h and 12 h after treatment (data not shown) and we could not observe obvious differences between expression profiles obtained from two independent samples treated with an identical cytokine (data not shown), data extensively obtained at earlier and later time points at multiple concentrations of cytokines may provide findings to reveal the kinetics of modulation in gene expression after the cytokine stimulation.

The results shown here indicate that our approach of analyzing the cellular responses of HCAECs to five individual cytokines from the novel standpoint of similarity and diversity in the alteration of gene expression levels is capable of identifying new description and classification of the constituents of the cellular response. Previously, several studies were conducted with DNA microarrays for analyzing the alteration of gene expression in endothelial cells after stimulation with cytokines [5–7]. Among them, the most minutely conducted study reported on the identification of the expression levels that altered in a TNF- α and IFN- γ -specific manner from the expression profiles obtained with five species of endothelial cells and three individual inflammatory cytokines (TNF- α , IFN- γ , and IL-4), a total of 15 individual samples analyzed in parallel [6]. In addition, the authors paid attention to the tissue specificity of endothelial cells and the functional specificity among three individual cytokines and isolated marker genes for individual cytokine function in respective species of endothelial cells. Similar to this report, most of

the previous studies focused on identifying markers specific to stimulation or to tissues and cells. In contrast, we at first focused on analyzing minutely the cellular responses solely described with gene expression ratios prior to identifying the specific marker genes. The 15 response patterns found in this study (response patterns A~O) consist of genes belonging to various categories in the biological process outlined by GO in a response pattern-specific manner (Table 3). Thus, it is possible to remark that these response patterns are characterized by itself with a constitution of the numbers and species of genes included.

In this study, we chose cytokines as representative factors to stimulate endothelial cells. Endothelial cells respond to cytokines present in local microenvironments through altering gene expression. The cellular response induces a variety of alterations such as the promotion of the recruiting of immune cells via surface molecules expressed on the endothelial cells, increase in vascular permeability, and proliferation or apoptosis of the endothelial cells themselves [25–28]. However, endothelial cells should respond not only to secretory factors like cytokines but to humoral factors that derived exogenously such as endotoxins [29] and physical factors such as shear stress [30]. Therefore, in order to understand comprehensively the diversity of the response of endothelial cells, it is essential to systematically study the responses induced by diverse stimulations including physical, chemical, and biological factors. To achieve these systematic collections of cellular samples after various stimulations, it should be inevitable to comparatively analyze in parallel a great number of expression profiles on an identical platform. Our microarray system used in this study may contribute to establishing such a systematic analysis for the response of endothelial cells to the diverse stimulation since our system successfully analyzed 130 expression profiles in parallel [12].

Dysfunctions of endothelial cells are profoundly associated with a variety of pathological processes such as disseminated intravascular coagulation [31] and tumor progression [32]. Although focused studies have been conducted on these diseases recently, the pathological mechanism of these diseases and the response of endothelial cells involved in the mechanism are not fully understood. Comparative analysis in parallel for comprehensive gene expression profiles obtained with DNA microarrays from endothelial cells enables us to investigate the response of endothelial cells to a variety of exogenous stimulations from an extensive and minute standpoint. We expect that it may be contributable to the analysis of genes in such a way that it facilitates the understanding of the response of endothelial cells that are peculiar to vascular diseases and help in the invention of novel therapeutic targets for these diseases.

Acknowledgements: This work was supported by the grant “Functional Analysis of Protein and Research Application” from the New Energy and Industrial Technology Development Organization (NEDO), Japan. We thank Dr. Y. Kawamura at Japan Biological Information Research Center for bioinformatics study.

Appendix A. Supplementary data

Supplementary data associated with this article can be found, in the online version, at doi:10.1016/j.febslet.2006.11.041.

References

- [1] Cines, D.B. et al. (1998) Endothelial cells in physiology and in the pathophysiology of vascular disorders. *Blood*, 91, 3527–3561.
- [2] Rodgers, G.M. (1988) Hemostatic properties of normal and perturbed vascular cells. *FASEB J.* 2, 116–123.
- [3] Edgington, T.S. (1995) Vascular biology: integrative molecular cell biology. *FASEB J.* 9, 841–842.
- [4] Barton, M. (2000) Endothelial dysfunction and atherosclerosis: endothelin receptor antagonists as novel therapeutics. *Curr. Hypertens. Rep.* 2, 84–91.
- [5] Murakami, T. et al. (2000) The gene expression profile of human umbilical vein endothelial cells stimulated by tumor necrosis factor alpha using DNA microarray analysis. *J. Atheroscler. Thromb.* 7, 39–44.
- [6] Sana, T.R., Janatpour, M.J., Sathe, M., McEvoy, L.M. and McClanahan, T.K. (2005) Microarray analysis of primary endothelial cells challenged with different inflammatory and immune cytokines. *Cytokine* 29, 256–269.
- [7] Zhao, B., Stavchansky, S.A., Bowden, R.A. and Bowman, P.D. (2003) Effect of interleukin-1beta and tumor necrosis factor-alpha on gene expression in human endothelial cells. *Am. J. Physiol. Cell Physiol.* 284, 1577–1583.
- [8] Eder, J. (1997) Tumor necrosis factor alpha and interleukin 1 signalling: do MAPKK kinases connect it all? *Trends Pharmacol. Sci.* 18, 319–322.
- [9] Takaoka, A. and Yanai, H. (2006) Interferon signalling network in innate defence. *Cell Microbiol.* 8, 907–922.
- [10] Heinrich, P.C., Behrmann, I., Haan, S., Hermans, H.M., Muller-Newen, G. and Schaper, F. (2003) Principles of interleukin (IL)-6-type cytokine signalling and its regulation. *Biochem. J.* 374, 1–20.
- [11] Ito, E. et al. (2003) A tetraspanin-family protein, T-cell acute lymphoblastic leukemia-associated antigen 1, is induced by the Ewing’s sarcoma-Wilms’ tumor 1 fusion protein of desmoplastic small round-cell tumor. *Am. J. Pathol.* 163, 2165–2172.
- [12] Sakamoto, A. et al. (2005) Influence of inhalation anesthesia assessed by comprehensive gene expression profiling. *Gene* 356, 39–48.
- [13] Mantovani, A., Garlanda, C., Introna, M. and Vecchi, A. (1998) Regulation of endothelial cell function by pro- and anti-inflammatory cytokines. *Transplant. Proc.* 30, 4239–4243.
- [14] Samuel, C.E. (2001) Antiviral actions of interferons. *Clin. Microbiol. Rev.* 14, 778–809.
- [15] Sen, G.C. (2001) Viruses and interferons. *Annu. Rev. Microbiol.* 55, 255–281.
- [16] Brown, T.J., Rowe, J.M., Liu, J.W. and Shoyab, M. (1991) Regulation of IL-6 expression by oncostatin M. *J. Immunol.* 147, 2175–2180.
- [17] Modur, V., Feldhaus, M.J., Weyrich, A.S., Jicha, D.L., Prescott, S.M., Zimmerman, G.A. and McIntyre, T.M. (1997) Oncostatin M is a proinflammatory mediator. In vivo effects correlate with endothelial cell expression of inflammatory cytokines and adhesion molecules. *J. Clin. Invest.* 100, 158–168.
- [18] Wahl, A.F. and Wallace, P.M. (2001) Oncostatin M in the anti-inflammatory response. *Ann. Rheum. Dis.* 60, 75–80.
- [19] Vasse, M., Pourtau, J., Trochon, V., Muraine, M., Vannier, J.P., Lu, H., Soria, J. and Soria, C. (1999) Oncostatin M induces angiogenesis in vitro and in vivo. *Arterioscler. Thromb. Vasc. Biol.* 19, 1835–1842.
- [20] Dinarello, C.A., Gelfand, J.A. and Wolff, S.M. (1993) Anticytokine strategies in the treatment of the systemic inflammatory response syndrome. *JAMA* 269, 1829–1835.
- [21] Sen, G.C. and Lengyel, P. (1992) The interferon system. A bird’s eye view of its biochemistry. *J. Biol. Chem.* 267, 5017–5020.
- [22] Peri, S. et al. (2003) Development of human protein reference database as an initial platform for approaching systems biology in humans. *Genome Res.* 13, 2363–2371.
- [23] Briones, M.A., Phillips, D.J., Renshaw, M.A. and Hooper, W.C. (2001) Expression of chemokine by human coronary-artery and umbilical-vein endothelial cells and its regulation by inflammatory cytokines. *Coron Artery Dis.* 12, 179–186.
- [24] Krishnaswamy, G., Smith, J.K., Mukkamala, R., Hall, K., Joyner, W., Yerra, L. and Chi, D.S. (1998) Multifunctional cytokine expression by human coronary endothelium and regulation by monokines and glucocorticoids. *Microvasc Res.* 55, 189–200.

- [25] Harlan, J.M. (1985) Leukocyte–endothelial interactions. *Blood* 65, 513–525.
- [26] Breslin, J.W., Pappas, P.J., Cerveira, J.J., Hobson 2nd., R.W. and Duran, W.N. (2003) VEGF increases endothelial permeability by separate signaling pathways involving ERK-1/2 and nitric oxide. *Am. J. Physiol. Heart Circ. Physiol.* 284, 92–100.
- [27] Takahashi, H., Numasaki, M., Lotze, M.T. and Sasaki, H. (2005) Interleukin-17 enhances bFGF-, HGF- and VEGF-induced growth of vascular endothelial cells. *Immunol. Lett.* 98, 189–193.
- [28] Chen, J., Li, D., Zhang, X. and Mehta, J.L. (2004) Tumor necrosis factor-alpha-induced apoptosis of human coronary artery endothelial cells: modulation by the peroxisome proliferator-activated receptor-gamma ligand pioglitazone. *J. Cardiovasc. Pharmacol. Ther.* 9, 35–41.
- [29] Dauphinee, S.M. and Karsan, A. (2006) Lipopolysaccharide signaling in endothelial cells. *Lab. Invest.* 86, 9–22.
- [30] Passerini, A.G., Milsted, A. and Rittgers, S.E. (2003) Shear stress magnitude and directionality modulate growth factor gene expression in preconditioned vascular endothelial cells. *J. Vasc. Surg.* 37, 182–190.
- [31] Risberg, B., Andreasson, S. and Eriksson, E. (1991) Disseminated intravascular coagulation. *Acta. Anaesthesiol. Scand. Suppl.* 95, 60–71.
- [32] Le, A., Querrec, Duval, D. and Tobelem, G. (1993) Tumour angiogenesis. *Baillieres Clin. Haematol.* 6, 711–730.

Original Paper

Effusion and solid lymphomas have distinctive gene and protein expression profiles in an animal model of primary effusion lymphoma

Y Yanagisawa,¹ Y Sato,² Y Asahi-Ozaki,² E Ito,¹ R Honma,¹ J Imai,¹ T Kanno,² M Kano,² H Akiyama,² T Sata,² F Shinkai-Ouchi,³ Y Yamakawa,³ S Watanabe¹ and H Katano^{2*}

¹Department of Clinical Informatics, Tokyo Medical and Dental University, Tokyo, Japan

²Department of Pathology, National Institute of Infectious Diseases, Tokyo, Japan

³Department of Biochemistry and Cell Biology, National Institute of Infectious Diseases, Tokyo, Japan

*Correspondence to:

Dr H Katano, Department of Pathology, National Institute of Infectious Diseases, 1-23-1 Toyama, Shinjuku, Tokyo 162-8640, Japan.
E-mail: katano@nih.go.jp

Abstract

Lymphoma usually forms solid tumours in patients, and high expression levels of adhesion molecules are observed in these tumours. However, Kaposi's sarcoma-associated herpesvirus (KSHV)-related primary effusion lymphoma (PEL) does not form solid tumours and adhesion molecule expression is suppressed in the cells. Inoculation of a KSHV-associated PEL cell line into the peritoneal cavity of severe combined immunodeficiency mice resulted in the formation of effusion and solid lymphomas in the peritoneal cavity. Proteomics using two-dimensional difference gel electrophoresis and DNA microarray analyses identified 14 proteins and 105 genes, respectively, whose expression differed significantly between effusion and solid lymphomas. Five genes were identified as having similar expression profiles to that of lymphocyte function-associated antigen 1, an important adhesion molecule in leukocytes. Among these, coronin 1A, an actin-binding protein, was identified as a molecule showing high expression in solid lymphoma by both DNA microarray and proteomics analyses. Western and northern blotting showed that coronin 1A was predominantly expressed in solid lymphomas. Moreover, KSHV-encoded lytic proteins, including viral interleukin-6, were highly expressed in effusion lymphoma compared with solid lymphoma. These data demonstrate that effusion and solid lymphomas possess distinctive gene and protein expression profiles in our mouse model, and suggest that differences in gene and protein expression between effusion and solid lymphomas may be associated with the formation of effusion lymphoma or invasive features of solid lymphoma. Furthermore, the results obtained using this combination of proteomics and DNA microarray analyses indicate that protein synthesis partly reflects, but does not correlate strictly with, mRNA production. Copyright © 2006 Pathological Society of Great Britain and Ireland. Published by John Wiley & Sons, Ltd.

Keywords: primary effusion lymphoma; animal model; proteomics; DNA microarray; Kaposi's sarcoma-associated herpesvirus

Received: 26 December 2005
Revised: 7 March 2006
Accepted: 17 April 2006

Introduction

Primary effusion lymphoma (PEL), also known as body cavity-based lymphoma (BCBL), is a rare complication in patients with acquired immunodeficiency syndrome (AIDS) [1–4], and has a unique character compared with other types of lymphoma. While all other types of lymphoma form solid tumours in lymph nodes or extranodal sites, PEL cells proliferate in the peritoneal, abdominal or pericardial cavity of patients as lymphomatous effusions [2]. Curiously, PEL rarely progresses to leukaemia, and PEL cells prefer to grow as effusions in these body cavities [2]. PEL is known to be associated with Kaposi's sarcoma-associated herpesvirus (KSHV, human herpesvirus 8) infection [1,2,4]. KSHV-encoded latency-associated nuclear antigen (LANA, ORF73) is detected

in the nucleus of almost all PEL cells, suggesting that KSHV infects PEL cells in the latent phase [5–7]. KSHV infection is also associated with a type of solid lymphoma (KSHV-associated solid lymphoma) [5,8], which occurs in the skin, lungs and gastrointestinal tract of AIDS patients with homosexual behaviour and sometimes complicates other KSHV-associated diseases, such as Kaposi's sarcoma, PEL, and multicentric Castleman's disease [5]. Since KSHV-associated solid lymphoma possesses similar expression profiles of cellular and viral proteins to PEL, KSHV-associated solid lymphoma is thought to be an extra-cavity variant of PEL [8,9]. Although the molecular biological differences between PEL and KSHV-associated solid lymphoma remain unknown, PEL shows some unique characteristics in its clinical course compared with KSHV-associated solid lymphoma. For example, PEL

cells do not usually demonstrate marked invasion of the peritoneal or pleural membrane, whereas KSHV-associated solid lymphoma often exhibits massive invasion of other organs [2,8–10]. Although the role of KSHV in the formation of solid or effusion lymphoma is currently unknown, the expression of adhesion molecules, such as lymphocyte function-associated antigen type 1 (LFA-1), is likely to be essential for solid lymphoma formation [11–13].

In general, adhesion molecules are expressed on the surface of almost all types of lymphoma cell [13,14]. LFA-1 is the most important molecule involved in lymphocyte adhesion. Almost all leukocytes express LFA-1 on their cell surface, and its mechanism of activation has been elucidated in T cells. Briefly, LFA-1 is activated by stimulation of Rap 1-RAPL from T cell receptors [15], and also by chemokines through the small GTPase RhoA and atypical zeta protein kinase C [16]. When LFA-1 becomes activated, it moves on the cell surface (polarization and redistribution) [17]. Expression of LFA-1 has been reported in various other cell types, including lymphoma cells [18,19]. Epstein–Barr virus-encoded latent membrane protein 1 up-regulates LFA-1 in infected cells [19–21]. Some adult T cell leukaemia cells show low expression of the LFA-1 β -chain (CD18) [22,23]. Thus, some viral infections regulate the expression of LFA-1, although the mechanism of this regulation remains unknown. Since LFA-1 expression is down-regulated in PEL cell lines [11,24–26], this suppression of LFA-1 expression should contribute to the unique features of PEL.

Here, we established an animal model that produced both effusion and solid lymphomas from a KSHV-associated PEL cell line [10]. Using proteomics and DNA microarray analyses, we investigated the differences in the gene and protein expression profiles between effusion and solid types of KSHV-associated lymphoma in this animal model.

Materials and methods

Inoculation of the PEL cell line TY-1 into severe combined immunodeficiency (SCID) mice

TY-1 [27], a KSHV-positive PEL cell line, was injected into the abdominal cavity of 8–10-week-old CB-17 SCID mice [10]. A total of 1×10^7 cells was inoculated into each mouse. All animal procedures were approved by the Animal Care and Use Committee of the National Institute of Infectious Diseases (NIID, Approval No 205 091), and were conducted according to 'the Guidelines for Animal Experiments Performed at the NIID'.

Two-dimensional difference gel electrophoresis (2D-DIGE)

2D-DIGE, gel image analysis and matrix-assisted laser desorption ionization/time-of-flight (MALDI-ToF) mass spectrometry were performed as described [28–30]. Details of these procedures are described in

the supplementary material (<http://www.interscience.wiley.com/jpages/0022-3417/suppmat/path.2012.html>).

RNA preparation and DNA microarray

RNA preparation and DNA microarray analysis (MicroDiagnostic, Tokyo, Japan) was performed as previously described [31,32] (supplementary methods, available at <http://www.interscience.wiley.com/jpages/0022-3417/suppmat/path.2012.html>).

Western blotting

Cell extract preparation and immunoblotting analyses were performed as described [5]. Aliquots of 50 μ g protein/lane were separated by sodium dodecyl sulphate–polyacrylamide gel electrophoresis (SDS–PAGE), and probed with anti-LFA-1 (BD Biosciences Pharmingen, San Diego, CA, USA), anti-coronin (Upstate Biotechnology, Lake Placid, NY, USA), anti-vIL-6 [5], anti-ORF59 [5] or anti-Lyn (Santa Cruz Biotechnology, Santa Cruz, CA, USA) antibodies.

Real-time PCR

The amounts of KSHV mRNA and DNA were determined by quantitative real-time (TaqMan) polymerase chain reaction (PCR) using an ABI Prism 7900 HT sequence detection system (Applied Biosystems, Foster City, CA, USA) as described [33–35]. The probe sequences, primer sequences, and real-time PCR details are described in the supplementary methods available at <http://www.interscience.wiley.com/jpages/0022-3417/suppmat/path.2012.html>.

Results

Establishment of an animal model for effusion and solid lymphomas

We previously reported that inoculation of a PEL cell line, TY-1, resulted in solid lymphoma formation in the peritoneal cavity of SCID mice (Figure 1A) [10,27]. Some of these SCID mice also showed effusion lymphoma formation in their peritoneal cavity. We separately collected both effusion and solid lymphoma components, and inoculated effusion lymphoma cells into the peritoneal cavity of some SCID mice and solid lymphoma cells into subcutaneous sites of other SCID mice. After 3–4 weeks, the effusion lymphoma-inoculated mice showed ascites including effusion lymphoma, whereas the solid lymphoma-inoculated mice developed subcutaneous tumours composed of TY-1 cells. These lymphomas were transplanted six times until the 7th passage (Figure 1B). During the passages, inoculation of effusion lymphoma cells into the peritoneal cavity formed not only effusion lymphoma but also solid lymphoma in the

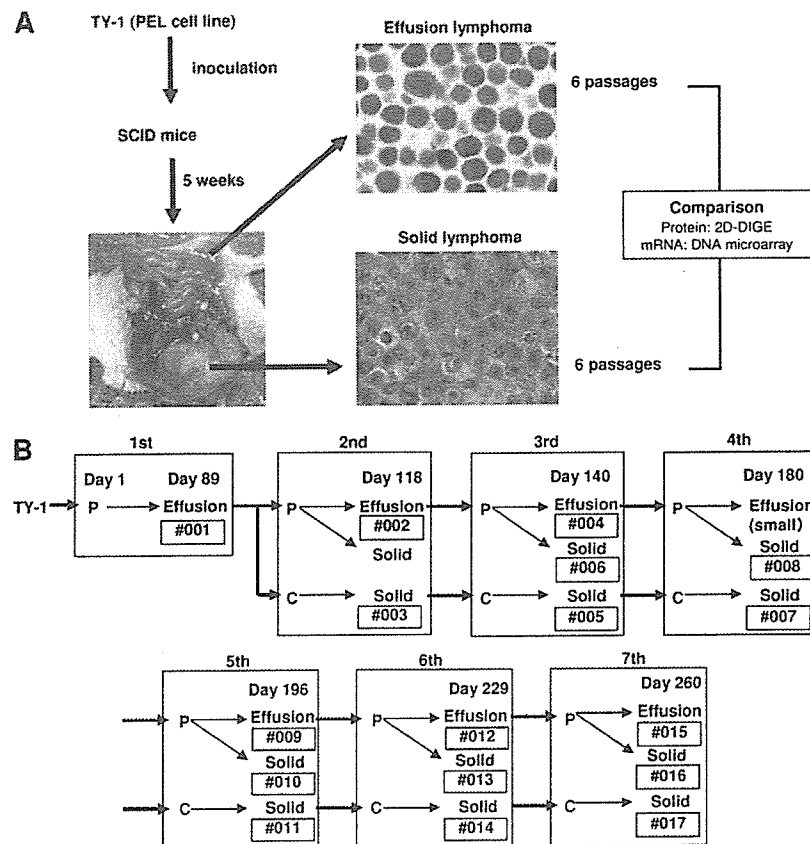


Figure 1. Animal model of effusion and solid lymphomas. (A) Experimental procedure. TY-1, a PEL cell line, was inoculated into the peritoneal cavity of SCID mice. After 5 weeks, effusion and solid lymphomas were obtained from the cavity. These lymphomas were inoculated into other SCID mice. Finally, the protein and gene expression profiles of the two types of lymphoma were compared by 2D-DIGE (proteomics) and DNA microarray analyses. (B) Passages and sample numbers in the present study. Inoculation of effusion lymphoma into other SCID mice resulted in the formation of not only effusion lymphoma but also solid lymphoma in the peritoneal cavity. Samples were taken from both and the sample numbers are shown as #001–017. P = peritoneal cavity; C = subcutaneous

peritoneal cavity in some mice (sample Nos 6, 8, 10, 13, and 16 in Figure 1B). The solid lymphoma-inoculated mice did not develop effusion lymphoma in any of their cavities. Immunohistochemistry revealed that both the effusion and solid lymphomas in SCID mice expressed hCD45, hCD30, and KSHV-LANA [10,36], indicating that the origin of the lymphoma cells was TY-1 [27].

Proteomics of effusion and solid lymphomas

To investigate the differences in the protein expression profiles between effusion and solid lymphomas, effusion and solid lymphoma cells of the 2nd, 3rd, 5th, and 6th passages (sample Nos 2, 4, 9, and 12 [effusion] and 3, 5, 11, and 14 [solid] in Figure 1B, respectively) were collected and lysed in lysis buffer. The lysates were labelled with CyDyes and applied to 2D-DIGE [29]. DeCyder, an image analysis software program, identified 23 spots as proteins showing differences in expression between effusion and solid lymphomas. Among these, 14 and nine spots

were identified as proteins showing higher expression in solid and effusion tumours, respectively. All 23 spots were excised from the gels after staining with Coomassie brilliant blue. The proteins in these spots were digested with trypsin, and identified by MALDI-ToF mass spectrometry (Figure 2). Finally, eight and seven proteins were identified as showing higher expression in effusion and solid lymphomas, respectively (supplementary Table 1 at <http://www.interscience.wiley.com/jpages/0022-3417/suppmat/path.2012.html>). One of these was a mouse protein, but the others were all of human origin. The proteins in the other eight spots could not be identified by mass spectrometry owing to their low levels.

Differential analysis using a DNA microarray

mRNA was extracted from effusion and solid lymphoma samples (sample Nos 1–14), and differences in the mRNA expression profiles were investigated using a DNA microarray containing 28 654 human genes. The DNA microarray identified 105 genes whose

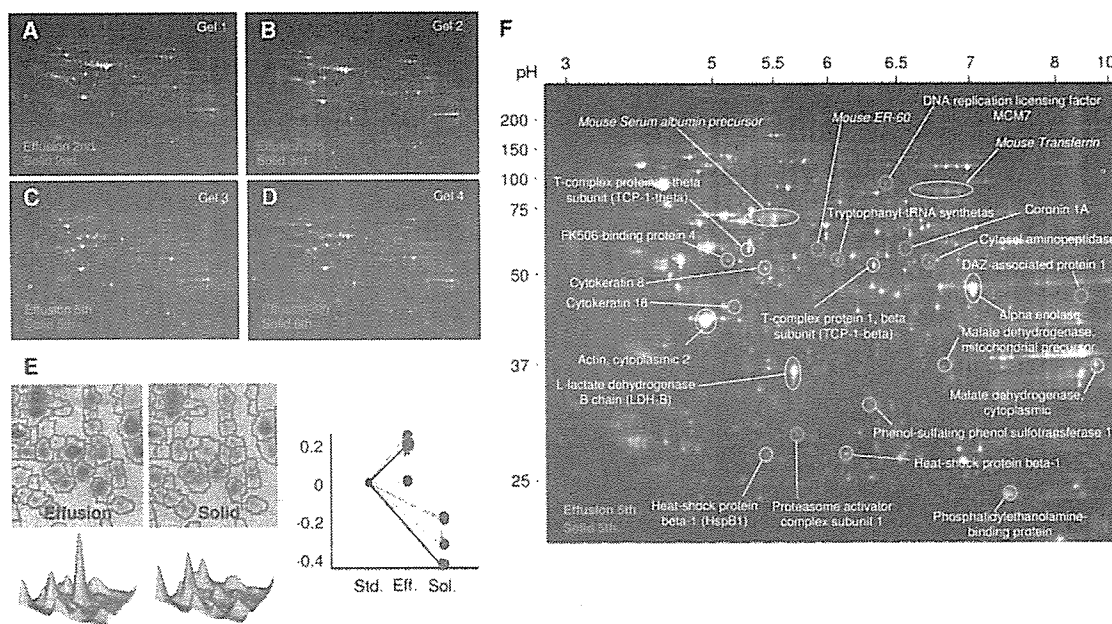


Figure 2. Proteomics of effusion and solid lymphomas. (A–D) Images of 2D-DIGE for the 2nd, 3rd, 5th, and 6th passages of the lymphomas. Proteins from effusion lymphoma were labelled with Cy2 (green) in gel 1 (2nd passage) and gel 3 (5th passage), but Cy3 (red) in gel 2 (3rd passage) and gel 4 (6th passage). Proteins from solid lymphoma were labelled with different colours from effusion lymphoma. (E) Examples of computerized analysis using the DeCyder™ software. The software automatically recognizes all the protein spots on the 2D-DIGE images (upper panels). It then calculates the peak of each protein and draws three dimensional images (lower panels). The peaks were automatically compared among the four gels. Finally, a graph of the protein expression levels in effusion and solid lymphomas (right panel) is created. See text and ‘Supplementary methods’ (<http://www.interscience.wiley.com/jpages/0022-3417/suppmat/path.2012.html>) for details. (F) Images of 2D-DIGE and results of MALDI-ToF mass spectrometry. Green and red circles indicate protein spots showing significantly higher expression in effusion and solid lymphomas, respectively. Yellow circles indicate protein spots showing similar expression in both effusion and solid lymphomas

expression differed by more than two-fold between solid and effusion lymphomas with *p*-values of <0.005 by *t*-tests (Figure 3A and supplementary data at <http://www.interscience.wiley.com/jpages/0022-3417/suppmat/path.2012.html>). Among these, 49 and 56 genes were identified as showing higher expression in effusion and solid lymphomas, respectively (supplementary Table 2 at <http://www.interscience.wiley.com/jpages/0022-3417/suppmat/path.2012.html>). The group showing predominant expression in effusion lymphoma contained transactivator/cell cycle-associated genes (MAPKAPK2, C/EBPD, G protein-coupled receptor, RRAS, etc), enzymes (ATPase, arginase, lipase, etc), and a cell surface antigen (CD68) (Table 1). The group showing predominant expression in solid lymphoma contained structural proteins (collagens, proteoglycans), adhesion molecules (integrins) and cell cycle-associated genes (MAPKs, IRF1, etc.). In particular, several kinds of collagen were identified as genes predominantly expressed in solid lymphoma.

Comparison of the proteomics and DNA microarray results

Some molecules were identified by both the proteomics and DNA microarray analyses. However, there were also discrepancies between the two sets

of results. Therefore, we compared the mRNA levels identified by the DNA microarray and the protein levels identified by the proteomics analysis (supplementary Table 1 at <http://www.interscience.wiley.com/jpages/0022-3417/suppmat/path.2012.html>). The human proteins with higher expression in solid lymphoma identified by the proteomics analysis (Nos 1–4, 6, and 7 in supplementary Table 1) showed similar expression patterns in the DNA microarray. In contrast, only six of eight proteins with higher expression in effusion lymphoma identified by the proteomics analysis (Nos 8–15 in supplementary Table 1) showed similar trends in the DNA microarray (Nos 9–11 and 13–15). Thus, although the two assays produced similar trends between the two lymphomas, suggesting that mRNA expression correlated with expression of the corresponding proteins, some of the differences in mRNA production detected between the two groups were not significant at the protein level, suggesting that protein expression did not correlate fully with the production of mRNA for these proteins.

Molecules with similar expression profiles to LFA-1

LFA-1 is a major adhesion molecule in lymphocytes [13,14], and its down-regulation plays an

Table 1. Summary of gene and protein expression between effusion and solid lymphomas

	Higher expression in effusion lymphoma	Higher expression in solid lymphoma
Structural or matrix protein	Mucins, JVA	Collagens, CSPG2, LOXLI, SPARC , BGN, <i>Coronin</i> , AEBP1, H1FO
Transactivator Cell cycle-associated	MAPKAPK2, C/EBPD, RAS	MAPKs, IGFBP7, IRF1, <u>MCM7</u>
Cell surface membrane protein	CD68, cathepsin B, EMPI, DAF, CAV1, GPR25,	ITM2C, Integrins (ITGAM, LFA-1), FUT7
Enzymes	DHRS3, ATPase, arginase, lipase, <u>P-PST</u> , malate dehydrogenase, <u>FK506-BP4</u>	ADA, ACY-3, PTP4A3, ATP2A1, PLCG2, <u>TrpRS</u> , <u>LAP</u>
Others	<u>HSP27</u> , keratins, <u>PEBP</u> , etc	RBPI , SQLE , C4B, DAZ-associated protein, <u>PA28a</u> , etc

Genes/proteins identified as showing higher expression in effusion or solid lymphomas are listed. Genes/proteins with unknown function are not listed. Proteins identified by proteomics are underlined. Italics indicate genes/proteins identified by both DNA microarray and proteomics. Bold indicates genes with similar expression profiles to LFA-1.

important role in the pathogenesis of PEL [11]. Immunohistochemistry detected no LFA-1 expression in effusion lymphoma and relatively high expression in solid lymphoma (Figures 4A and B). We attempted to identify genes with similar expression patterns to LFA-1. Cluster analysis of the DNA microarray results based on expression of the 105 identified genes revealed that at least five of the genes belonged to the same cluster as LFA-1 (Figure 3B), suggesting that they had similar expression profiles to LFA-1. Among these five genes, coronin 1A was also identified by proteomics as a protein showing high expression in solid lymphoma. Thus, we investigated the expression of LFA-1 and coronin 1A in effusion and solid lymphomas (Figure 4). Western blotting demonstrated that both LFA-1 and coronin 1A expression was increased during passages in solid lymphoma (Figure 4C). Effusion lymphoma did not express LFA-1, but showed weak expression of coronin 1A (Figure 4C). Northern blot analysis demonstrated that coronin 1A was expressed in solid lymphoma, but not in effusion lymphoma (Figure 4D). These data suggest that coronin 1A has a similar expression profile to LFA-1 in this animal model of effusion and solid lymphomas.

Viral gene and protein expression

Next, we investigated the expression of KSHV-encoded genes and proteins. Real-time PCR analysis demonstrated that the viral interleukin (vIL)-6 transcript showed approximately seven-fold higher expression in effusion lymphoma than in solid lymphoma (Figure 4F). The mRNA copy numbers for ORF50 and ORF73 were also higher in effusion lymphoma than in solid lymphoma (Figures 4E and G). The viral load of KSHV was investigated by real-time PCR analysis for ORF26 DNA (Figure 4H). The results demonstrated that the viral genome titres were lower in solid lymphoma than in effusion lymphoma. Western blotting showed that vIL-6 was only expressed in effusion lymphoma, while LFA-1 and coronin 1A were predominantly expressed in solid lymphoma. The expression

of ORF59, a lytic protein of KSHV, decreased during the passages, but did not differ significantly between effusion and solid lymphomas (Figure 4C). Northern blotting also revealed a high level of vIL-6 expression in effusion lymphoma (Figure 4D). Although LANA was expressed in both effusion and solid lymphomas throughout all passages by immunohistochemistry (data not shown), these data suggest that KSHV was activated in effusion lymphoma, but not in solid lymphoma.

Discussion

PEL has unique features compared with all other subtypes of lymphoma [2,4], since its growth is usually restricted to one body cavity and it does not develop into leukaemia or metastasis. Although PEL cells show slight invasion of body cavity walls, such as the pleural or peritoneal membrane, marked invasion and solid tumour formation are rarely found. These features of PEL are dependent on the low expression of adhesion molecules [11,24–26]. Low or absent adhesion molecule expression should contribute to the formation of such an effusion phenotype. On the other hand, KSHV-associated solid lymphoma progresses rapidly and invades various organs, such as the gastrointestinal tract, lungs, and skin [8–10]. Thus, these two lymphomas have distinctive clinical courses, although their cells show similar protein expression patterns, suggesting an identical origin [8,9]. In the present study, 105 of 28 654 genes in a DNA microarray were identified as genes showing differences in expression between effusion and solid lymphomas. Proteomics also identified 14 proteins with differences in expression between the two lymphomas. Therefore, although our data showed that the cellular gene expression profiles of these two lymphomas were very similar, distinctive expression profiles of some genes and proteins were identified between effusion and solid lymphomas in our mouse model. Since the KSHV-associated solid lymphoma cells used in our mouse